Detection Theory and Industrial Applications
Final Project
Gestaltic Grouping of Line Segments

David Faget Caño
david.faget_cano@ens-paris-saclay.fr

February 2024

1 Introduction

The papers [9] and [10] under study discuss the application of Gestalt theory in computer vision, particularly focusing on the detection of meaningful geometric structures in digital images through Gestalt principles. Gestalt theory, originating in the early 20th century, proposed a set of laws such as similarity, proximity, connectedness, and good continuation (GC) to explain how humans group visual elements to perceive objects. While these laws were initially qualitative, there have been efforts to quantitatively formalize them for use in computer vision.

The discussed research concentrates on using the *a contrario* model, a method based on the principle of non-accidentalness. This principle suggests that a structure in an image is considered meaningful if its parts are too regularly arranged to be a coincidence. Since its origins, the *a contrario* model has been applied to various tasks, including detecting point alignments for vanishing point estimation, automatic line segment detection with linear time complexity, and identifying circles, ellipses, good continuations, and image corners.

Furthermore, the *a contrario* framework has been utilized in image matching algorithms, object recognition, and image segmentation, emphasizing the detection of non-accidental structures as a way to segment and understand images. The papers [9] and [10] highlight the use of line segments detected by an automatic line segment detector (in this case, LSD [4]) as basic elements for forming more complex Gestalt groups, such as long straight lines and parallel segments. This approach is noted for its efficiency, leveraging the fewer, more structured line segments compared to the vast number of unstructured image pixels, facilitating lower time complexity in detecting meaningful geometric patterns in images. The analogy of this work as a step up in a pyramid is represented in Figure 1.

Since the paper is very complete and very close to what is asked for the project, the objective of this report will not only be to explain the paper. Instead, we will try to bring something new to it, and to discuss it under a critical point of view. Therefore, we will start Section 2 by giving the definition of the problem and by linking it to the Gestalt theory seen in class. Then, we will formally formulate the problem in Section 3 and we will give algorithms and experimental results in Section 4. Finally, Section 5 will be dedicated to discuss possible improvements and extensions.

2 Definition of the Problem and Link with Gestalt Theory

Informal Definition of the Problem

In [9], authors build upon the "partial Gestalts" identified by the Line Segment Detector (LSD) to investigate their potential as foundational elements for constructing more complex Gestalt groups, such as long straight lines, good continuations, and parallel line segments. As mentionned in the introduction, they employ an *a contrario* framework on the line segments distribution, utilizing it to systematically identify the aforementioned structures as non-random occurrences. Addressing this problem is important because line segments play a key

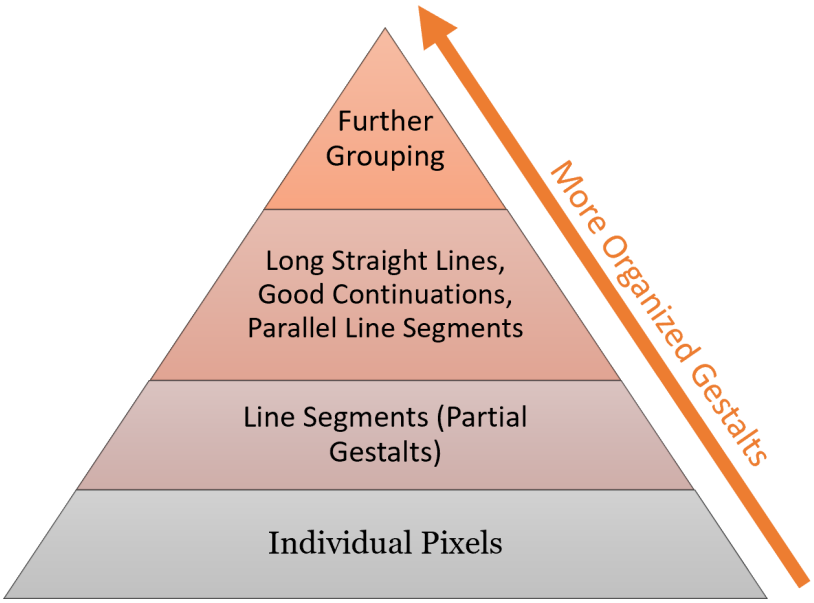

Figure 1: The analogy with a bottom-up pyramid involves constructing a hierarchical structure for feature extraction from images, starting with the simplest elements and progressively moving towards more complex structures. The passage from the base to the first floor is performed by algorithms such as LSD. In this project, we mainly study the passage from the first floor to the second floor. Future research should study the transition from the second to the third floor.

role in revealing the geometric aspects of images. By organizing these segments into coherent structures, we can gain deeper insights into the images' composition.

Link with Gestalt Theory

Gestalt theory is a psychological approach that emphasizes the idea that the whole of anything is greater than its parts. Originating in the early 20th century with German psychologists, including Max Wertheimer, Kurt Koffka, and Wolfgang Köhler, Gestalt psychology focuses on how people perceive and process visual information and suggests that humans naturally perceive objects as organized patterns and wholes, rather than as separate components. Key principles are vicinity, similarity, continuity of direction, amodal completion, closure, constant width, tendency to convexity, symmetry, common motion, and past experience, which explain how we group elements during perception. Essentially, Gestalt theory proposes that our minds are structured to organize sensory information into a unified whole, leading to the perception of order in what might otherwise be chaotic stimuli.

In the context of grouping line segments together, Gestalt theory suggests that our minds naturally organize these segments into meaningful patterns rather than seeing them as disconnected elements. For instance, when we look at a series of lines, we might perceive a shape or a whole object. This is because our perception leans towards simplifying and organizing visual information into a unified form, making sense of the segments in relation to each other and the larger whole they suggest, rather than focusing on each individual part.

In paper [9], authors focus on three Gestalt groups of line segments: non-local alignments, bars and good continuations. As seen in class, the law of good continuation can be stated as "All else being equal, elements that can be seen as smooth continuations of each other tend to be grouped together" [7] (p. 259). Intuitively, non-local alignments correspond to long straight lines, while bars match with parallel line segments. We will

give formal definitions and visual examples of these three Gestalt groups in the next section.

3 Formal Formulation of the Problem

3.1 The *a contrario* Model

As seen in class, the *a contrario* (or background) model H_0 is the stochastic model that is implicitly assumed when we say "explained by chance". In terms of our problem, let's examine a collection of N oriented line segments, denoted as $l_1, l_2, \ldots, l_N$, located within a rectangular area measuring n by m. According to [9], "the adopted a contrario model H_0 is a set of N stochastic line segments, with independent and uniformly distributed tips on the image domain". We are going to delve deeper into this sentence.

First, as described above, it is clear that the background model must take into account the line segments detected by a fixed algorithm (in the case of the paper, it is the LSD algorithm). But here the term stochastic does not mean that line segments are detected in a stochastic manner (many algorithms designed for detecting line segments such as LSD are deterministic). Instead, it refers that the tips of the line segments follow a probability distribution on the image domain. And this probability distribution is assumed to be uniform, together with the assumptions that tips are independent. This assumption simplifies the model, but does not take into account that real-world images often have regions with varying feature densities. It also ignores the spatial relationships between line segments, such as parallelism or contiguity, common in structured environments. However, it is a common assumption in many related problems, such as good continuation detection in point patterns seen in class and in paper [5].

3.2 Definition of the Events and Tests

Good Continuation, Non-local Alignment and Bar

Let's begin this section by highlighting a key distinction from the scenario of event detection (such as GC) in point patterns. In those cases, points did not have an inherent direction. In contrast, when considering segments, their orientation becomes a crucial factor. As a consequence, the formal definition of the events we will deal here with oriented segments. The following definitions are extracted from [9].

In the next definition, $D(\cdot)$ and $\angle(\cdot)$ denote respectively the maximum of the distances and the maximum of the angles between successive oriented line segments in a sequence. The two threshold values ρ and θ limit the search space around each line tip for finding close line segments. A small fixed margin is also allowed to deal with possible misalignments in the LSD outputs. Since the goal of this project is not to reformulate paper [9], some details may be ignored.

Definition 1 (Good Continuation (GC)) *A sequence of k line segments $l_{a_1}, l_{a_2}, \ldots, l_{a_k}$ form a potential good continuation event $\wp^{k,\rho,\theta}$ if and only if $D(l_{a_1}, l_{a_2}, \ldots, l_{a_k}) < \rho$ and $\angle(l_{a_1}, l_{a_2}, \ldots, l_{a_k}) < \theta$ for predefined constant ρ and θ thresholds.*

Definition 2 (Non-local Alignment (NLA)) *A good continuation with $\theta = 3^\circ$ is called a non-local alignment event $\zeta^{k,\rho}$.*

In the following definition, $D_m(\cdot)$ represents the mutual distance operator, which is determined by calculating the greatest distance between the corresponding ends of the two line segments that form the bar. The parameter $\Delta\theta$ is introduced to address the effects of sampling in digital images. As we commented before, it is important to note that the orientation of the line segments is taken into account when calculating $D_m(\cdot)$. Specifically, the first end of line segment l_i is matched with the second end of line segment l_j, and the reverse is also true.

Definition 3 (Bar) *Two line segments or non-local alignments l_i and l_j are said to form a bar $\Im^\rho$ if and only if $D_m(l_i, l_j) < \rho$ and $\pi - \Delta\theta \leq \angle(l_i, l_j) \leq \pi + \Delta\theta$ for $\Delta\theta = 3^\circ$ and ρ is a predefined constant threshold.*

Notice in particular that a line segment can belong simultaneously to several of these higher order groups of Gestalts. For example, all line segments belonging to NLA also belong to GC, since NLA is a particular case of GC where segments form (approximately) a straight line.

Figure 2 provides some visual toy examples of these events.

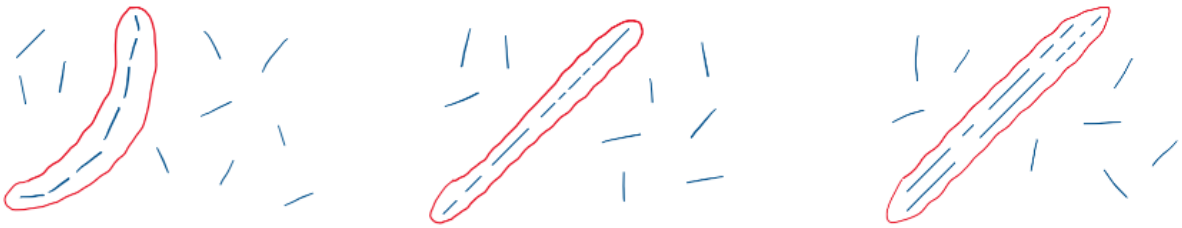

Figure 2: Visual representation of the events considered in this project. From left to right: events surrounded in red are a Good Continuation, a Non-local Alignment and a Bar (formed by two non-local alignments)

The Number of Tests

Let's denote N_{test} the number of possible occurrences of an event e. Since we are dealing with segments, we will have

$$N_{test} = c_e \cdot M_e$$

where c_e and M_e depends on e. If $e \in \{GC, NLA\}$ then M_e is the number of all possible sequences of k line segments out of overall N line segments. Therefore,

$$M_e = \frac{N!}{(N-k)!}$$

Now, if $e = Bar$, we have that $M_{Bar} = \frac{N(N-1)}{2}$.

For the calculation of c_e, we must explore the three events of interest independently. First, for c_{GC}, to prioritize smoother continuations with closer tips, rather than relying on a single set of ρ and θ thresholds in the calculation, we introduce n_ρ and n_θ predefined thresholds. For each promising continuation chain, we determine the smallest pair of (ρ_i, θ_j) where $D(l_i, l_{i+1}, \ldots, l_j) < \rho_i$ and $\angle(l_i, l_{i+1}, \ldots, l_j) < \theta_j$ before computing the N_{test}. This pair is then utilized in the formula. Accounting for the maximum number K of line segments in a chain, we set $c_{GC} = K \cdot n_\rho \cdot n_\theta$. For c_{NLA}, we notice that $c_{NLA} = c_{GC}$ since NLA are a particular case of GC and they can be as numerous as GC instances. Finally, we have that $c_{Bar} = n_\rho$ since (like for GC) the ρ threshold is tested over n_ρ different values.

3.3 Number of False Alarms (NFA)

As precised in the lecture notes [6], the name NFA is justified by the following fact: a candidate c_i in data x with $NFA(c_i, x) = \alpha$ will be validated as a detection only if ε is larger than or equal to α, and in such case the method will get at most α false detections. In other words, $NFA(c_i, x)$ corresponds to the false detection level needed to accept the event. Moreover, an event e is ε-meaningful if $NFA(e) \leq \varepsilon$.

Here, we observe a slight difference between lecture notes [6] and the paper [9]. In the latter, meaningfulness is defined when $NFA(e) < \varepsilon$, without considering the case $NFA(e) = \varepsilon$. However, in the following, we will follow [9] notation, since this difference is not relevant in practice. The constant ε corresponds to the expected number of false detections that one is ready to accept, which depends on the task being handled. In [9], authors fix $\varepsilon = 1$. As seen in [6], this is a common convention already proposed by Desolneux et al. in [2].

Paper [9] defines the NFA as the stochastic expectation of an event e, and therefore $NFA(e) = N_{test} \cdot P_{H_0}(e)$, where the term on the right is the probability of the geometric event under H_0. This formulation is coherent

with the one given in lecture notes [6]. A large NFA means that the event is to be expected under the *a contrario* model and is therefore too frequent to be of interest. On the other hand, a small NFA corresponds to a rare event and therefore arguably a meaningful one

In order to compute the NFA in the case of GC, for the probability term $P_{H_0}(\wp^{k,\rho,\theta})$ authors of [9] assume uniform independent distribution of line segment endpoints and uniform distribution of line angles throughout the image domain. The first assumption was already discussed when we introduced the *a contrario* model. However, these assumptions face limitations due to boundary effects, making them not simultaneously realizable. Particularly, boundary effects constrain the spatial distribution of line segment tips, violating the uniformity assumption near the image edges. Although these assumptions are not strictly applicable across the entire image domain, they are considered a valid approximation for line segments of limited length in large image domains, where boundary effects have a diminished impact on the overall distribution of line segments and their orientations.

Details of the calculation of the NFA are given in [9]. Notice that for NLA, we set $\theta = 0.05$, which is $3°$. The obtained expressions are the following:

$$\mathrm{NFA}^{GC}(k,\rho,\theta) = K \cdot n_\rho \cdot n_\theta \cdot \frac{N!}{(N-k)!} \cdot \left(\frac{\theta\rho^2}{mn} \cdot \frac{\theta}{\pi}\right)^{k-1}$$

$$\mathrm{NFA}^{NLA}(k,\rho) = K \cdot n_\rho \cdot n_\theta \cdot \frac{N!}{(N-k)!} \left(\frac{2\lambda\rho}{mn} \cdot \frac{\theta}{\pi}\right)^{k-1}$$

$$\mathrm{NFA}^{Bar}(\rho) = n_\rho \cdot \frac{N(N-1)}{2} \left(\frac{\Delta\theta\rho^2}{mn}\right)^2$$

3.4 Examples and Analysis of the NFA

We observe that $\mathrm{NFA}^{Bar}(\rho)$ is proportional to more of the fourth power of ρ. This means that when we increase the tolerated distance, the NFA gets much bigger. In other words, fixed ε, the more we increase the distance between the two segments (or NLA) forming the bar, the less likely is for the event to be meaningful. This aligns with our intuition. Specifically, when observing a picture featuring parallel lines, those that are positioned closer to each other tend to attire more our attention.

The same reasoning can be done for GC, with a slight difference. In this case, the NFA depends on three parameters: k, ρ and θ. We observe that the greater are these parameters, the less likely are the events to be meaningful. Notice that the distance and the angles contribute equally to the meaningfulness of the event, since they are raised to the same power. A similar reasoning can be done in the case of NLA.

We are going to give now a toy example of a calculation of the NFA. Suppose that we fix $\varepsilon = 1$, $\Delta\theta = 0.087(5°)$ and that we are in a square domain of dimensions $32 \cdot 32$. Suppose also that we have two parallel segments out of overall $N = 10$ segments, and that $n_\rho = \rho$. Then, what should be the value of the distance ρ between these segments to be considered as meaningful? We would have

$$\mathrm{NFA}^{Bar}(\rho) \approx \rho^5 \cdot 3.25 \cdot 10^{-7}$$

Therefore, we find that $NFA(\rho) < 1$ if, approximately, $\rho < 19.8$. This means, for example, that if we had two parallel segments at each border of the square domain, there would not be considered as meaningful, since they would be too far from each other.

4 Algorithms and Experiments

4.1 Explanation of the Algorithms

Two main algorithms are presented in paper [9]. The first one detects GC, and the second one detects Bars (remember that NLA are a particular case of GC). In this subsection, we will explain briefly these algorithms, without giving details, since they are provided in the paper under study.

GC Detection Algorithm

The algorithm identifies good continuations in a set of line segments based on connectivity, smoothness, and length. It operates in three main steps:

Inputs: Line segments with their coordinates, and parameters (ρ, θ, K) controlling maximum distance and angle between segments, and maximum length of continuations.

1. Adjacency Matrix: Creates a matrix to identify segments close enough (under ρ and θ) to be potentially connected.
2. Find Chains: Detects all possible sequences of up to K segments that could represent continuous paths.
3. Select Good Continuations: Sorts these chains by NFA and selects the best as good continuations.

Output: A list of these good continuations, each a sequence of line segments that together form a visually smooth and connected path.

Bar Detection Algorithm

This algorithm detects bars within a set of line segments and non-local alignments based on distance and angular alignment:

Inputs: Line segments and non-local alignments with their coordinates, a maximum distance (ρ), and an angle threshold ($\Delta\theta$).

Process: Combines segments and alignments, checks each pair for distance less than ρ and alignment within $\Delta\theta$, and evaluates their potential as bars using a significance measure.

Output: A list of bars, each a pair of line segments that meet the distance and alignment criteria, ensuring they are significant and distinct.

The algorithm focuses on identifying pairs of segments that align closely to form bars, based on predefined proximity and angular criteria.

4.2 Non-Redundant Detections

Let's dedicate this section to discuss about if it is worth to apply an exclusion principle in this case, and about analyzing the redundancy of the detections. As seen in [6], the heuristic approach utilized by LSD addresses the issue of redundancy by testing candidates that are line-support regions, which emerge from a specific segmentation of the input image. This approach ensures that line segment candidates do not overlap, eliminating redundant detections. This ensure that the input segments are non-redundant. However, in the case of GC in point patterns seen in [6], we noted that a good continuation event might mask another smaller event contained in itself (e.g. a subset of the points in a meaningful chain can be also meaningful). The general idea in that case [6] was to evaluate the chains in order, from the most meaningful (smallest NFA value) to the least meaningful one (largest NFA value). If a chain was not masked by any previously found chain, it was added to the output list, otherwise it was rejected. The same situation holds for our case, where the inputs are segments. This idea is implemented in the *SortChains* and *findGC* procedures of Algorithm 1 [9]. A similar idea is implemented for bar detection, avoiding redundant detections.

4.3 Experimental Results

All the experiments presented in this section have been done directly by using the paper [9] demo on the IPOL site.

A Simple Example

Initially, we will illustrate the use of the algorithm with a basic example, which will provide a foundation for the case of failure that we will present later. Notice that for this project, it does not make sense to take a random input image (with any meaningful structures) since no line segments would be detected. Let's consider the flat spiral presented in Figure 3, and apply the algorithm on it. The configuration employed is presented in Table 1, and results are shown in Figures 4 and 5. Detection statistics are presented in Table 2. The algorithm was successfully executed in 15.2s.

Figure 3: Orginal picture

Radius (in pixels)	Angle (in degrees)	Maximum number of segments
10	155	10

Table 1: Set of parameters for the simple example.

Type	**Number of detections**
Initial line segments	112
Good continuations	17
Parallelism	0
Non-local alignments	0
Residual (not grouped line segments)	4

Table 2: Detection statistics for the simple example.

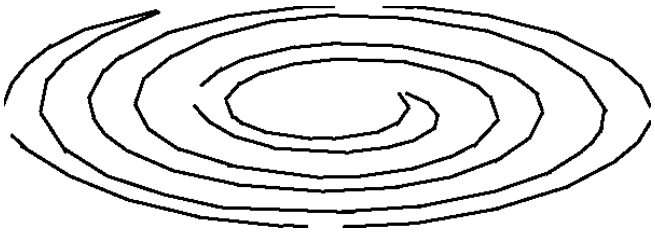

Figure 4: LSD

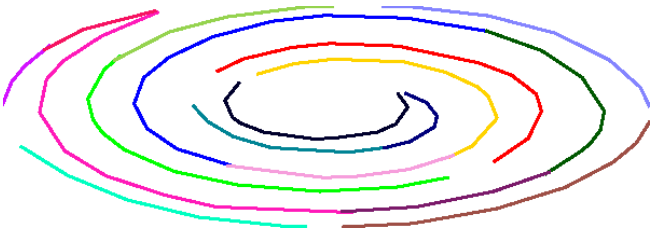

Figure 5: GC

We note that neither NLA nor bars are identified, which aligns with the fact that the spiral consists of neither straight nor parallel lines. According to what we visually perceive, almost all the input segments are classified as GC, except for four, which are considered residual. This outcome is consistent with our visual interpretation of the spiral, and serves as a first basic example of the application of the algorithm.

A More Complex Example

Here's a more detailed scenario for illustration. The algorithm is executed on photograph presented in Figure 6, which I captured in the library while studying. It has dimension 384x682 pixels, and it presents a notably complex and interesting case, given the multitude of segments created by the books and shelves.

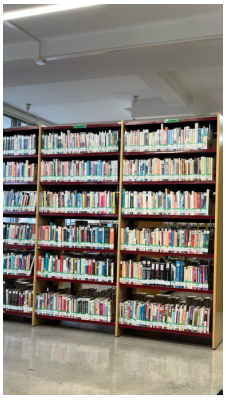

Figure 6: Orginal picture

I decided to execute the algorithm twice, with two different configurations, in order to analyze the differences. The first set of parameters chosen is presented in Table 3, and the results are shown in Figures 7 to 11. Table 4 contains the number of detections of segments and of each event, as well as the number of residual segments. The algorithm was successfully executed after 48.5s with this configuration.

Radius (in pixels)	Angle (in degrees)	Maximum number of segments
10	155	5

Table 3: First set of parameters used.

Type	**Number of detections**
Initial line segments	716
Good continuations	108
Parallelism	144
Non-local alignments	47
Residual (not grouped line segments)	200

Table 4: Detection statistics with the first configuration.

We observe that, overall, the results are satisfying. In the vast majority of cases, LSD only detect one segment for each book, which is what we expected. We can particularly observe that NLA are formed by the edges of the shelves (which are long straight lines, formed by several segments detected by LSD). Moreover, bars are principally formed by the parallel position of the books, which are close to each other. However, for GC, we observe some strange structures inside of the shelves, which are mainly formed by the contour of several books. In order to avoid them, I hypothesised that diminishing the angle in the parameters should help. This fact motivates the second set of parameters, presented in Table 5. The algorithm was executed after 50.4s with the second configuration. This is probably because we doubled the maximum number of segments. Results obtained are shown in Figures 12 to 16, and statistics are presented in Table 6.

Radius (in pixels)	Angle (in degrees)	Maximum number of segments
10	30	10

Table 5: Second set of parameters used.

Figure 7: LSD

Figure 8: GC

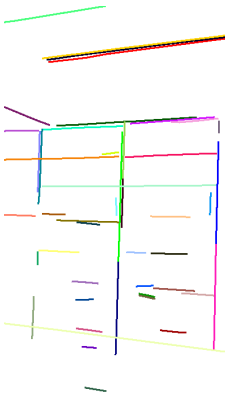

Figure 9: NLA

Figure 10: Bars

Figure 11: Res.

Type	**Number of detections**
Initial line segments	716
Good continuations	66
Parallelism	145
Non-local alignments	46
Residual (not grouped line segments)	259

Table 6: Detection statistics with the second configuration.

Figure 12: LSD

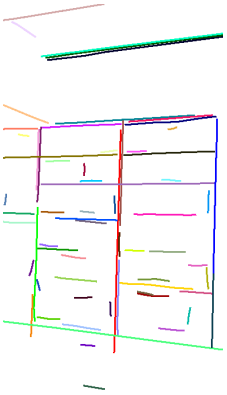

Figure 13: GC

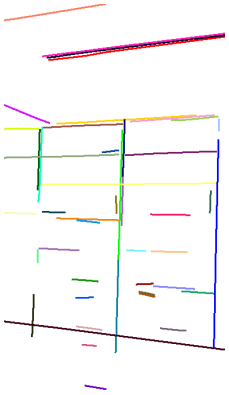

Figure 14: NLA

Figure 15: Bars

Figure 16: Res.

First, we observe that the input for our algorithm (line segments detected by LSD) is the same, since LSD is a deterministic algorithm. While detected NLA and bars are mainly the same, we observe a significant difference for GC. Indeed, since we are restricting the angle, we detect much less good continuations in the interior of the shelves, which is what we expected.

A Case of Failure

We are going to present now an interesting example, which will also motivate the next section in which we will discuss about improvements and extensions. It is clear that all the algorithms presented in paper [9] rely on the quality of the line segment detector algorithm. Therefore, if input line segments are not well detected, the results of the algorithms will be meaningless. The simple example presented in this section showed a spiral, for which LSD performed adequately. However, what would happen if we have an image with much less contrast? Figure 17 represents this situation. Human visual system sees a spiral without any difficulty (following Gestalt principles). However, as presented in Figure 18, LSD is not able to detect this structure. It might be assumed

that the difficulty in detecting the spiral arises from its curved nature as opposed to straight segments. However, the simple example demonstrates that this is not the case. The real challenge lies in the low contrast of the image, not the geometrical shape of the spiral itself. In conclusion, this is an interesting case of failure due to the dependency on LSD.

Figure 17: Original photo

Figure 18: LSD

5 Improvements and Extensions

Returning to the pyramid illustrated in Figure 1, we focus on the step involving "Long Straight Lines, Good Continuations, Parallel Line Segments". The aim of the algorithms mentioned in [9] is to identify these patterns. This section is dedicated to exploring potential enhancements and extensions, beginning with examining the detection of line segments, moving one step down, and finally discussing additional grouping strategies, moving one step up in the pyramid.

5.1 One Step Down: Changing The Line Segment Detector Algorithm

The first possible enhancement one could think is changing the line segment detector algorithm. Indeed, LSD algorithm was published more than one decade ago, and many advancements and deep learning techniques have emerged since then. Nonetheless, as we'll explore in this section, the LSD algorithm may still be the preferable option for our needs. Its low complexity and high accuracy render it particularly apt for addressing our specific problem. We will base our answer in a very recent and interesting benchmark of line segment detectors [3] done by Thibaud Ehret and Jean-Michel Morel. This section could be very extensive and be the subject of a whole project, and as a consequence, we will only give arguments of why LSD stills a good choice and provide some visual examples of it.

The first argument that supports the use of LSD is its fast execution. Table 7 shows that LSD is nowadays the fastest line segment detector algorithm. Since the algorithms under study in this paper depend on the line segment detector in order to pass from the original image to Gestaltic groups of segments, this is a crucial criterion.

LSD	ED-Lines	SOLD2	M-LSD	TP-LSD	ULSD	LETR
0.065	0.093	15.108	4.342	31.421	8.132	9.089

Table 7: Table given in [3], where the execution times (in seconds) of various algorithms applied to the same image are compared.

The second argument is that even if some algorithms could perform slightly better than LSD, they are not

perfect. Figure 19 shows the result of applying DeepLSD [8] on the spiral of Figure 17 (where we discussed the case of failure). We observe that it also fails to capture the structure that we, as humans, perceive.

Figure 19: DeepLSD applied to Figure 17.

5.2 One Step Up: What Comes Next ?

To address the figure-background problem effectively using unsupervised algorithms, it is necessary to enhance bottom-up grouping strategies. Specifically, curves that exhibit good continuation but are interrupted by gaps need to be bridged using irregular contours. Additionally, discrepancies in good continuations or alignments should be accounted for by incorporating T-junctions. Furthermore, instances of bars and non-local alignments can be reorganized according to principles of good continuation and parallelism. These advanced grouping techniques are essential for refining the separation of figures from their background in an unsupervised manner. Related papers such as [1] discuss how to detect structures like contours, corners and T-junctions.

6 Conclusion

Our observations across various images reveal that, aside from a minimal number of residual line segments, the algorithm effectively categorizes all line segments, thereby contributing to a further level of the segmentation pyramid. This enhances the comprehensive analysis and interpretation of the structural composition of images. A key benefit of this methodology lies in its efficient time complexity, achieved by leveraging line segments as the primary input, which are significantly fewer in quantity compared to the vast, unorganized collection of all pixels in an image. However, the performance of the algorithm could be negatively impacted by its reliance on the line segment detector it utilizes. This opens the door to future research, where enhancing line segment detection and further grouping could potentiate the applicability of the algorithms analyzed in this project.

References

[1] Buades, A., G. v. G. R. . N. J. Joint Contours, Corner and T-Junction Detection: An Approach Inspired by the Mammal Visual System. *J Math Imaging 60* (2018), 341–354. https://doi.org/10.1007/s10851-017-0763-z.

[2] Desolneux, A., Moisan, L., and Morel, J.-M. *From Gestalt Theory to Image Analysis: A Probabilistic Approach*, vol. 34. 01 2008.

[3] Ehret, T., and Morel, J.-M. Line Segment Detection: a Review of the 2022 State of the Art. *Image Processing On Line 14* (2024), 41–63. https://doi.org/10.5201/ipol.2024.481.

[4] Grompone von Gioi, R., Jakubowicz, J., Morel, J.-M., and Randall, G. LSD: a Line Segment Detector. *Image Processing On Line 2* (2012), 35–55. https://doi.org/10.5201/ipol.2012.gjmr-lsd.

[5] Lezama, J., Randall, G., Morel, J.-M., and Grompone von Gioi, R. An Unsupervised Algorithm for Detecting Good Continuation in Dot Patterns. *Image Processing On Line 7* (2017), 81–92. https://doi.org/10.5201/ipol.2017.176.

[6] Morel, J.-M., and Grompone von Gioi, R. *Detection Theory and Industrial Applications.* Lecture Notes.

[7] Palmer, S. *Vision Science: Photons to Phenomenology.* MIT Press, 1999.

[8] Pautrat, R., Barath, D., Larsson, V., Oswald, M. R., and Pollefeys, M. Deeplsd: Line segment detection and refinement with deep image gradients, 2023.

[9] Rajaei, B., and Grompone von Gioi, R. Gestaltic Grouping of Line Segments. *Image Processing On Line 8* (2018), 37–50. https://doi.org/10.5201/ipol.2018.194.

[10] Rajaei, B., von Gioi, R. G., and Morel, J.-M. From line segments to more organized gestalts. In *2016 IEEE Southwest Symposium on Image Analysis and Interpretation (SSIAI)* (2016), pp. 137–140.